Preprints (www.preprints.org) | NOT PEER-REVIEWED | Posted: 16 March 2020

Differential ceRNA Expression and Interaction Analysis in Coronary Artery Disease

Sheng Kang[1*#], Yong Ye[1#], Guang Xia[1], Haibo Liu[1,2*]

1. Department of Cardiology, Shanghai East Hospital, Tongji University, Jimo Road 150, Shanghai 200120, China.
2. Department of Cardiology, Qingpu Branch of Zhongshan Hospital, Fudan University, 1158 Park East Road, Shanghai 201700, China.

#Sheng Kang and Yong Ye were Co-first authors in the paper.

*Sheng Kang and Haibo Liu were Co-corresponding authors in the paper.

Corresponding authors: Sheng Kang, E-mail: kangsheng2008@163.com; Haibo Liu, E-Mail: haiboliu13@fudan.edu.cn

© 2020 by the author(s). Distributed under a Creative Commons CC BY license.

Preprints (www.preprints.org) | NOT PEER-REVIEWED | Posted: 16 March 2020

Abstract:

Previous studies had shown that mRNA, miRNA and lncRNA were associated with cardiovascular diseases. The study was aimed to explore the differential expressions of mRNA, lncRNA and miRNA between coronary artery disease (CAD) and healthy control, and their interaction in CAD. We investigated the differential expression of ceRNA between CAD and healthy control through data collected from Gene Expression Omnibus (GEO) microarrays. Furthermore, we investigated the biological function of these differential expressions of ceRNAs by Gene Ontology (GO), Kyoto Encyclopedia of Genes and Genomes (KEGG) analyses. Protein-protein interaction (PPI) network was created to identify the hub genes. Biosystems and literature search were performed for signaling pathways and their function of the included differential expression ceRNAs. A total of 456 miRNA expression profiles, 16,325 mRNA expression profiles, and 2,869 lncRNA expression profiles were obtained. Eleven Go and KEGG pathways (count ≥9), top 15 of PPI network node connectivity rank, and top 15 of ceRNA network node degree centrality rank were achieved at the statistical significance level ($P<0.05$). We further identified that several differential expressions of ceRNAs and their signaling pathways were associated with CAD through biosystems and literature search. Based on eleven Go and KEGG pathways, top 15 of PPI network node connectivity rank, and top 15 of ceRNA network node degree centrality rank in CAD population, our findings would contribute to further exploration for the molecular mechanism of CAD.

Key words: miRNA; lncRNA; mRNA; ceRNA; CAD

Preprints (www.preprints.org) | NOT PEER-REVIEWED | Posted: 16 March 2020

1. Introduction

Coronary artery disease (CAD) is a complex phenotype driven by genetic and environmental factors. However current therapies focus on addressing the role of cholesterol and lifestyle in CAD. Despite advances in the development of lipid-lowering therapies, clinical trials have shown that a substantial risk of cardiovascular disease persists after currently recommended medical therapy.[1] Stratification for subsequent coronary events among patients with CAD is of considerable interest because of the potential to guide secondary preventive therapies. Recently, eight microRNAs (miRNAs) were identified to facilitate acute coronary syndrome diagnosis.[2] Targeting Angptl3 messenger RNA (mRNA) retarded the progression of atherosclerosis and reduced levels of atherogenic lipoproteins.[3] The expressing 9p21.3-associated long non-coding RNA ANRIL induces risk CAD phenotypes in non-risk vascular smooth muscle cells.[4] So far, it is not clear the mechanism of these RNAs in CAD and their interaction.

Noticeably, the different types of RNA molecule competed to bind to miRNA, which reduced the inhibitory effect of miRNA targeting on its mRNA.[5] These competitive endogenous RNA (ceRNA) included various types of RNA transcripts, such as circular RNA (circRNA), long-chain non-coding RNA (lncRNA), pseudogenes and protein-encoded mRNA, which competed for miRNA through the "language" mediated by the miRNA response element (MRE).[6] After that, researchers used bioinformatics methods to predict ceRNA regulatory networks. The effect of ceRNA on the target gene and the dependence of ceRNA on miRNA would be verified at the experiments of proteins and RNAs, but the functional verification would be performed at the experiments of cells and animal models.

Thus, the study was aimed to explore the differential expressions of mRNA, lncRNA and miRNA between CAD and healthy control, and the

Preprints (www.preprints.org) | NOT PEER-REVIEWED | Posted: 16 March 2020

interaction of them, including constructure of ceRNA regulatory networks, which would contribute to the molecular mechanism of CAD.

2. Results

2.1. Basic Information Statistics of Differential Expression Analysis

As described in the Methods, a total of 456 miRNA expression profiles (supplementary Table1), 16,325 mRNA expression profiles (supplementary Table 2), and 2,869 lncRNA expression profiles were obtained (supplementary Table 3).

According to the set threshold, 18 differentially expressed miRNAs were finally obtained, including 16 down-regulated and 2 up-regulated (supplementary Table 4). a total of 92 differential lncRNAs were obtained, including 46 down-regulated and 46 up-regulated (supplementary Table 5).

A total of 610 differential mRNAs were obtained, including 244 down-regulated and 366 up-regulated (supplementary Table 6).

Based on the obtained differential miRNA, lncRNA and mRNA, the heat map was shown in Figure 1 and the volcano map was shown in Figure 2.

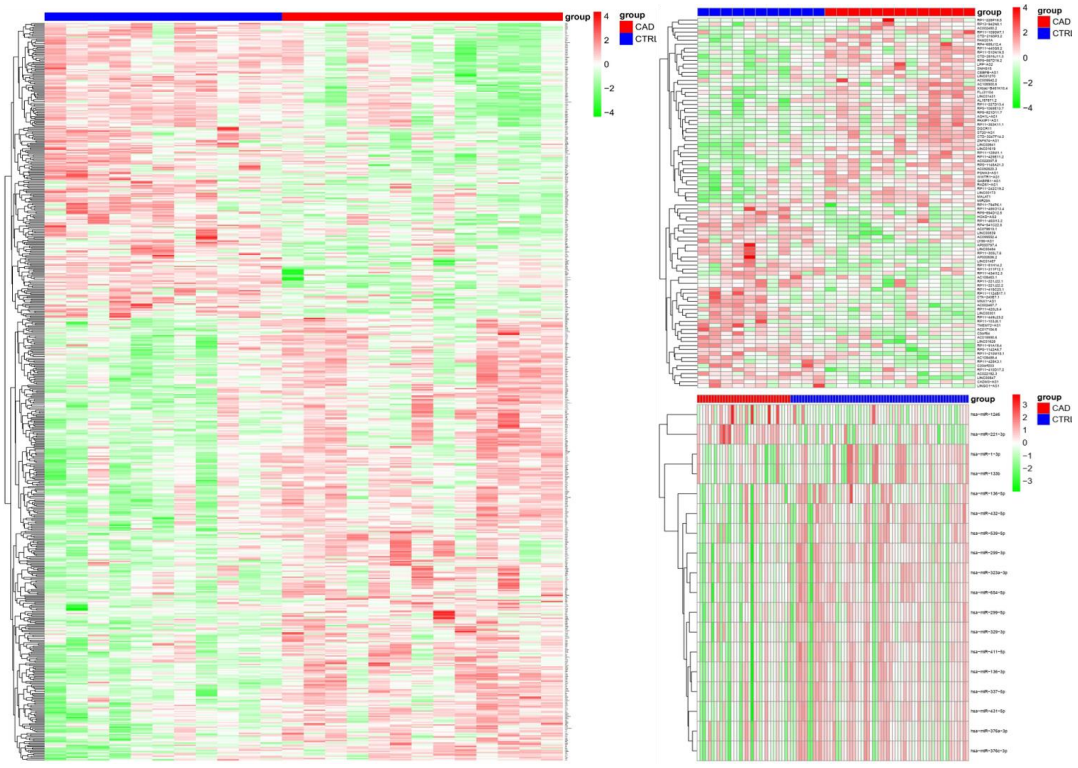

Figure 1. Heat map: Note: miRNA, lncRNA, and mRNA are presented from

Preprints (www.preprints.org) | NOT PEER-REVIEWED | Posted: 16 March 2020

left to right. Top red bar indicates the CAD samples, and blue bar indicates the control samples

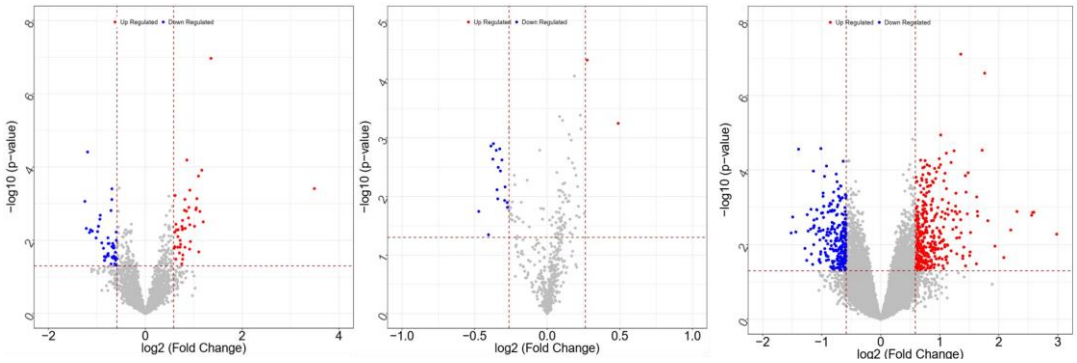

Figure 2. Volcano plot. Note: miRNA, lncRNA, and mRNA are displayed from left to right. Red indicates up-regulation, blue indicates down-regulation, grey indicates no significant difference.

2.2. Functional and Pathway Enrichment Analysis of Up- and Down-regulated MRNA

GOBP, GOMF, GOCC functional enrichment analysis and KEGG pathway enrichment analysis were performed on the obtained up-regulated and down-regulated mRNAs, respectively, and the results showed that a total of 36 GOBP, 3 GOCC, 15 GOMF and 2 KEGG pathways were significantly enriched (supplementary Table 7); Figure 3 presented only the TOP10 results, in accordance with ranking p value). The key results of GO and KEGG pathways enrichment analysis were displayed at Table 1.

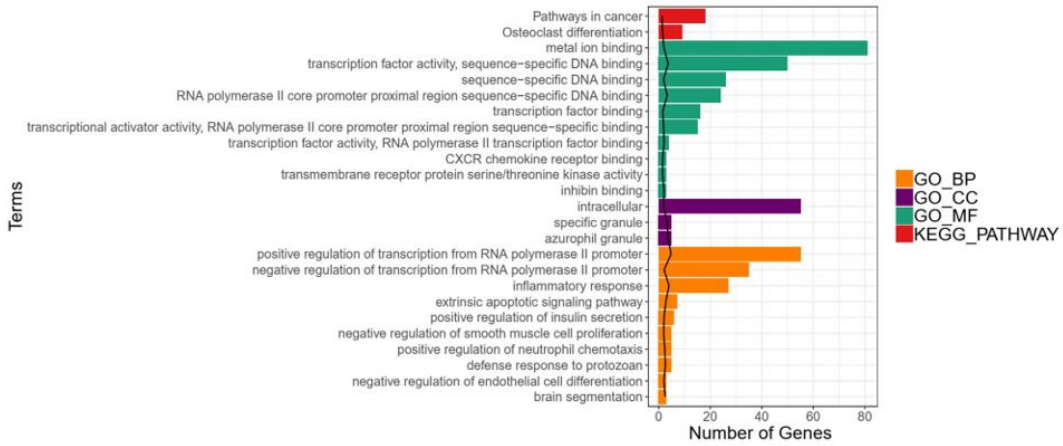

Figure 3. GO and KEGG PATHWAY enrichment analysis. Note: black lines indicate -log10 (p value), bar length indicates the number of enriched

Preprints (www.preprints.org) | NOT PEER-REVIEWED | Posted: 16 March 2020

genes.

Category	Term	Count	P Value
KEGG_PATHWAY	hsa04380: Osteoclast differentiation	9	2.82E-02
KEGG_PATHWAY	hsa05200: Pathways in cancer	18	4.33E-02
GOTERM_MF	GO: 0003700~transcription factor activity, sequence-specific DNA binding	50	1.77E-04
GOTERM_MF	GO: 0000978~RNA polymerase II core promoter proximal region sequence-specific DNA binding	24	4.40E-04
GOTERM_MF	GO: 0001076~transcription factor activity, RNA polymerase II transcription factor binding	4	7.53E-03
GOTERM_MF	GO: 0034711~inhibin binding	3	8.38E-03
GOTERM_MF	GO: 0046872~metal ion binding	81	8.79E-03
GOTERM_MF	GO: 0001077~transcriptional activator activity, RNA polymerase II core promoter proximal region sequence-specific binding	15	1.16E-02
GOTERM_MF	GO: 0043565~sequence-specific DNA binding	26	1.32E-02
GOTERM_MF	GO: 0008134~transcription factor binding	16	2.39E-02
GOTERM_MF	GO: 0004675~transmembrane receptor protein serine/threonine kinase activity	3	2.79E-02
GOTERM_MF	GO: 0045236~CXCR chemokine receptor binding	3	2.79E-02
GOTERM_CC	GO: 0042582~azurophil granule	5	2.18E-04
GOTERM_CC	GO: 0042581~specific granule	5	4.50E-04
GOTERM_CC	GO: 0005622~intracellular	55	1.28E-02
GOTERM_BP	GO:0045944~positive regulation of transcription from RNA polymerase II promoter	55	1.47E-05
GOTERM_BP	GO: 0006954~inflammatory response	27	9.45E-05
GOTERM_BP	GO: 0097191~extrinsic apoptotic signaling pathway	7	1.55E-03
GOTERM_BP	GO: 0042832~defense response to protozoan	5	2.23E-03
GOTERM_BP	GO: 0035284~brain segmentation	3	2.69E-03
GOTERM_BP	GO: 0090023~positive regulation of neutrophil chemotaxis	5	3.93E-03
GOTERM_BP	GO: 0000122~negative regulation of transcription from RNA polymerase II promoter	35	7.00E-03
GOTERM_BP	GO: 0032024~positive regulation of insulin secretion	6	7.58E-03
GOTERM_BP	GO: 0045602~negative regulation of endothelial cell differentiation	3	8.60E-03
GOTERM_BP	GO: 0048662~negative regulation of smooth muscle cell proliferation	5	1.08E-02

Table 1. Go and KEGG pathway enrichment analysis of differential genes

2.3. Protein Interaction Network Construction (PPI) and Module Analysis

As described in the methods, we achieved a total of 388 protein interaction

Preprints (www.preprints.org) | NOT PEER-REVIEWED | Posted: 16 March 2020

relationship pairs, and the network construction was performed using Cytoscape software as shown in Figure 4. A total of 171 nodes were included in the network.

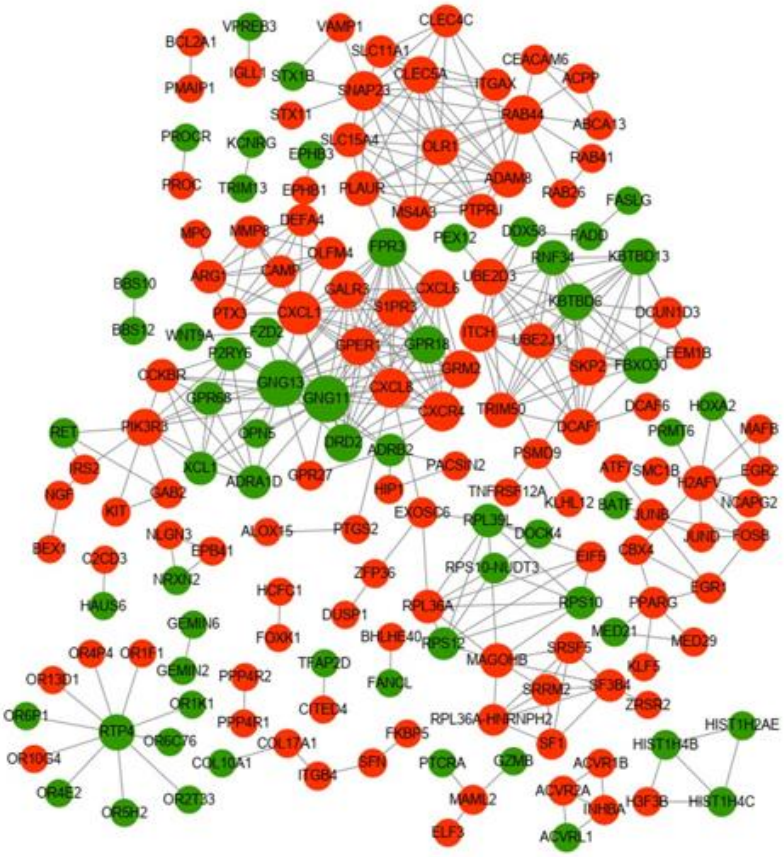

Figure 4. Protein interaction relationship network diagram (PPI). Note: red indicates up-regulated protein, green indicates down-regulated protein, gray line indicates protein interaction relationship, and node size indicates connectivity degree.

The network was analyzed for node connectivity according to the parameters set by the Method, the top15 of Degree Centrality (DC) of each node was ranked in Table 2. Notably, CXCL8, FPR2, IL6, and PPBP were ranked in Top15, which might be hub proteins in the network (supplementary Table 8). The top 15 of PPI network node connectivity rank were displayed at Table 2.

Node	Degree	P Value	TYPE	Name
GNG13	22	0.017945	DOWN	G protein subunit gamma 13

Preprints (www.preprints.org) | NOT PEER-REVIEWED | Posted: 16 March 2020

GNG11	22	0.04065	DOWN	G protein subunit gamma 11
CXCL1	18	0.000525	UP	C-X-C motif chemokine ligand 1
CXCR4	14	0.000134	UP	C-X-C motif chemokine receptor 4
CXCL8	14	0.001358	UP	C-X-C motif chemokine ligand 8
SNAP23	14	0.006229	UP	synaptosome associated protein 23
FPR3	13	0.003603	DOWN	formyl peptide receptor 3
RAB44	13	0.028049	UP	RAB44, member RAS oncogene family
SKP2	12	0.000943	UP	S-phase kinase associated protein 2
GPR18	12	0.001281	DOWN	G protein-coupled receptor 18
GALR3	12	0.001499	UP	galanin receptor 3
CXCL6	12	0.002672	UP	C-X-C motif chemokine ligand 6
ITCH	12	0.007857	UP	itchy E3 ubiquitin protein ligase
S1PR3	12	0.010344	UP	sphingosine-1-phosphate receptor 3
GRM2	12	0.010472	UP	glutamate metabotropic receptor 2

Table 2. PPI network node connectivity rank（TOP15）

2.4. MRNA and lncRNA Co-expression Analysis

We performed co-expression analysis of differentially expressed mRNAs and lncRNAs. According to the threshold set by the Methods, we screened a total of 1487 significantly coordinately expressed relationship pairs, including 381 mRNAs and 74 lncRNAs (supplementary Table 9)

2.5. MiRNA Target Genes and Upstream lncRNA Prediction Analysis

Based on the differentially expressed miRNAs and differential lncRNAs, a total of 452 lncRNA-miRNA relationship pairs were predicted as described in the Methods (supplementary Table 10), including 18 miRNAs, and 72 lncRNAs.

Also based on differentially expressed miRNAs, target gene prediction was performed using mirWalk as described in the Methods, after taking the intersection with the differential mRNAs, 276 miRNA-mRNA relationship pairs were obtained, including 17 miRNAs, and 170 mRNAs (supplementary Table 11)

2.6. Pathway Enrichment Analysis of lncRNAs and MiRNAs

As described in the Methods, a total of 27 lncRNAs were enriched by

Preprints (www.preprints.org) | NOT PEER-REVIEWED | Posted: 16 March 2020

KEGG pathway (supplementary Table 12) and 12 miRNAs were enriched by KEGG pathway (supplementary Table 13), here we showed a part of the results in Figure 5.

Figure 5. Results of lncRNA and miRNA pathway enrichment analysis. Note: top: lncRNA; bottom: miRNA; the decrease of significant p-value is shown from blue to red color, and bubble size indicates the proportion of

Preprints (www.preprints.org) | NOT PEER-REVIEWED | Posted: 16 March 2020

enriched genes (the number of involved term genes accounts for the number of input genes).

2.7. CeRNA Network Analysis

As described in the Methods section, based on the obtained miRNA-lncRNA and miRNA-mRNA relationship pairs, miRNA-lncRNA-mRNA relationship pairs regulated by the same miRNA were firstly screened, along with the positive co-expression relationship between mRNA and lncRNA (correlation coefficient>0.7), and lncRNA-miRNA-mRNA relationship pairs were further screened for network construction, i.e., the ceRNA network as shown in Figure 6.

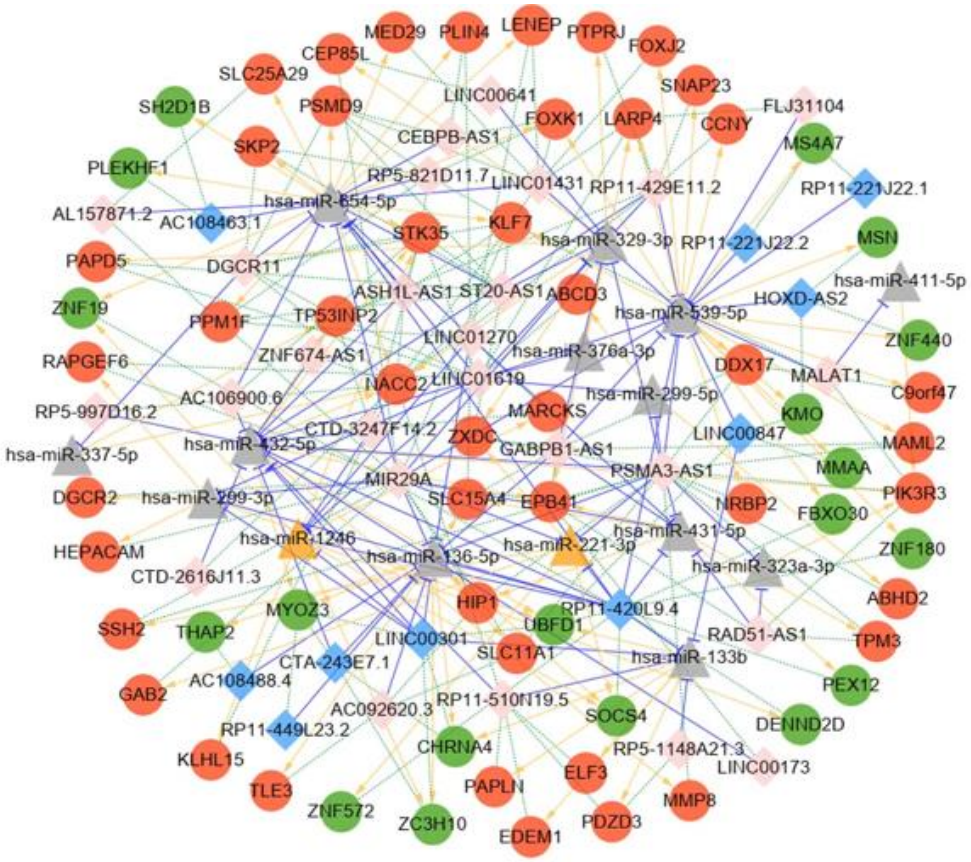

Figure 6. ceRNA network diagram. Note: the red circles represent up-regulated mRNAs, and green circles represent down-regulated mRNAs; yellow triangles represent up-regulated miRNAs, and gray triangles represent down-regulated miRNAs; blue diamond's represent

Preprints (www.preprints.org) | NOT PEER-REVIEWED | Posted: 16 March 2020

down-regulated lncRNAs, and pink diamonds represent up-regulated lncRNAs; The blue T-type lines represent the miRNA-lncRNA regulatory relationships, the yellow arrows represent the miRNA-mRNA regulatory relationships, and the green dotted lines represent the co-expression relationships of mRNA and lncRNA.

The network contained a total of 87 lncRNA-miRNA relationship pairs, 88 miRNA-mRNA relationship pairs, and 137 lncRNA-mRNA co-expression relationships (supplementary Table 14). There were a total of 36 lncRNAs, 64 mRNAs, and 15 miRNAs. Connectivity analysis was performed on each node of the ceRNA network to obtain mRNA, miRNA, and lncRNA connectivity as detailed in Table 3.

Node	Degree	Type	logFC	P Value
hsa-miR-539-5p	30	mi_down	-0.31167	0.002388
hsa-miR-654-5p	27	mi_down	-0.38709	0.001381
hsa-miR-432-5p	22	mi_down	-0.29313	0.011733
PSMA3-AS1	20	lnc_up	0.629594	0.032669
hsa-miR-136-5p	19	mi_down	-0.34012	0.010986
MIR29A	18	lnc_up	0.849701	0.001608
RP11-420L9.4	17	lnc_down	-0.69127	0.00077
LINC01619	14	lnc_up	0.610105	0.005996
NACC2	14	m_up	1.011445	7.23E-05
hsa-miR-329-3p	13	mi_down	-0.28995	0.006895
hsa-miR-1246	12	mi_up	0.489247	0.000567
hsa-miR-133b	11	mi_down	-0.40401	0.045067
hsa-miR-431-5p	11	mi_down	-0.37006	0.001259
ST20-AS1	10	lnc_up	1.167706	0.000122
STK35	10	m_up	1.147951	0.000764

Table 3. ceRNA network node degree centrality rank (TOP15)

3. Discussion

The study analyzed the differential genes at the statistical significance

Preprints (www.preprints.org) | NOT PEER-REVIEWED | Posted: 16 March 2020

level between CAD and healthy control, and found eleven Go and KEGG pathways (count ≥9), top 15 of PPI network node connectivity rank, and top 15 of ceRNA network node degree centrality rank, which would contribute to further exploration for the molecular mechanism of CAD.

Firstly, the Go and KEGG pathways (count ≥9) showed their function in Table 1, and they contained a large number of differential genes at the statistical significance level in CAD, thus these Go and KEGG pathways might play a role of molecular level of CAD. Several further explored experiments related to these pathways would achieve the interesting and important findings in CAD field.

Secondly, in top 15 of PPI network node connectivity rank, we found that the extensive protein interaction relationship pairs at the statistical significance level in CAD (Table 2), which matched with their signaling pathways in the biosystems (supplementary Table 15). Some of them were identified to play a role in cardiovascular diseases. For example, GNG11 was a member of the gamma subunit family of heteromeric G-protein. Overexpression of GNG11 activated ERK1/2 of the MAP kinase family, but did not Ras.[20] These findings provide clinically relevant biological insight into heritable variation in vagal heart rhythm regulation, with a key role for genetic variants (GNG11, RGS6) that influence G-protein heterotrimer action in GIRK-channel induced pacemaker membrane hyperpolarization (supplementary Table 15).[21]

CXCL1 was produced mainly by TNF-stimulated endothelial cells (ECs) and pericytes and supported luminal and sub-EC neutrophil crawling. CXCL1 and CXCL2 act in a sequential manner to guide neutrophils through venular walls as governed by their distinct cellular sources.[22] Angiotensin II-induced infiltration of monocytes in the heart is largely mediated by CXCL1-CXCR2 signalling which initiates and aggravates cardiac remodelling. Inhibition of CXCL1 and/or CXCR2 may represent new therapeutic targets for treating hypertensive heart diseases (supplementary Table 15).[23]

Wnt-Cxcr4 (C-X-C motif chemokine receptor 4) signaling in regulation of oligodendrocyte precursor cells (OPCs)-endothelial interactions coordinates OPC

Preprints (www.preprints.org) | NOT PEER-REVIEWED | Posted: 16 March 2020

migration with differentiation.[24] Many of the neutrophils reenter the vasculature and have a preprogrammed journey that entails a sojourn in the lungs to up-regulate CXCR4 before entering the bone marrow, where they undergo apoptosis.[25] Vascular CXCR4 limits atherosclerosis by maintaining arterial integrity, preserving endothelial barrier function, and a normal contractile SMC phenotype. Enhancing these beneficial functions of arterial CXCR4 by selective modulators might open novel therapeutic options in atherosclerosis (supplementary Table 15).[26]

Oleic acid treatment decreases the insulin sensitivity of heart muscle cells, and this sensitivity is completely restored by transfection with SNAP23. Thus, SNAP23 might be a link between insulin sensitivity and the inflow of fatty acids to the cell (supplementary Table 15).[27]

Co-activator-associated arginine methyltransferase 1 (CARM1) is a crucial component of autophagy in mammals. CARM1-dependent histone arginine methylation is a crucial nuclear event in autophagy, and identify a new signalling axis of AMPK-SKP2-CARM1 in the regulation of autophagy induction after nutrient starvation (supplementary Table 15).[28]

GPR18 is a cannabinoid-activated orphan G protein-coupled receptor (GPCR) that is selectively expressed on immune cells.[29] A salutary cardiovascular role for GPR18, mediated, at least partly, via elevation in the levels of adiponectin (supplementary Table 15).[30]

Thirdly, in top 15 of ceRNA network node degree centrality rank, the extensive ceRNA interaction relationship pairs at the statistical significance level in CAD (Table 3) , which matched with their description in the literature search (supplementary Table 16). Certainly, we also found that several ceRNA was related to cardiovascular diseases. For example, by regulating CDKN2A and inhibiting G1- to S-phase transition STK35L1 may act as a central kinase linking the cell cycle and migration of endothelial cells. The interaction of STK35L1 with nuclear actin might be critical in the regulation of these fundamental endothelial functions.[44] Serine/threonine kinase 35 (STK35) is a recently identified human kinase with an autophosphorylation function, linked functionally to actin stress fibers, cell

Preprints (www.preprints.org) | NOT PEER-REVIEWED | Posted: 16 March 2020

cycle progression and survival (supplementary Table 16).[45] Nuclear-retained importin α2 binds with DNase I-sensitive nuclear component(s) and exhibits selective upregulation of mRNA encoding STK35 by microarray analysis. Chromatin immunoprecipitation and promoter analysis demonstrated that importin α2 can access to the promoter region of STK35 and accelerate its transcription in response to hydrogen peroxide exposure. Furthermore, constitutive overexpression of STK35 proteins enhances caspase-independent cell death under oxidative stress conditions (supplementary Table 16).[46]

4. Materials and Methods

4.1. Data Preprocessing

miRNA expression profiling data were obtained from NCBI GEO (Gene Expression Omnibus, GEO, http://www.ncbi.nlm.nih.gov/geo/) database[7] to download the expression profile data after normalization of the dataset serial number GSE59421. A total of 96 samples with the subjects' characteristics (63 healthy controls (CTRL), 33 CAD blood samples), which were detected using the Agilent - 021827 Human miRNA MicroArray (V3) platform (miRBase release 12.0 miRNA ID version).

The mRNA/lncRNA data were also obtained from the NCBI GEO database to download the expression profile data after normalization of the dataset serial number GSE42148. A total of 24 samples with the subjects' characteristics (11 CTRL, 13 CAD blood samples), which were detected using the Agilent - 028004 SurePrintG3 Human GE 8 x 60K Microarray platform (Feature Number version).

4.2. MRNA and lncRNA Annotation

The sequences matched the probes of Agilent-028004 were obtained from the platform annotation file, and the human reference genome (GRCh38) sequences was downloaded from the GENCODE database[8] (https://www.gencodegenes.org/releases/current.html), and the probe sequences were aligned onto the reference genome using the seqmap software.[9] Firstly, we retained the uniquely aligned (unique map) probes,

Preprints (www.preprints.org) | NOT PEER-REVIEWED | Posted: 16 March 2020

and secondly, we referred their position to the chromosome with positive and negative strand information, the gene matched each probe was obtained according to the human gene annotation file (Release 25) provided by GENCODE.

We kept the probe with the annotating information "protein_coding" as the matching probe for mRNA, the probes with the annotating information with "antisense", "sense_intronic", "lincRNA", "sense_overlapping" or "processed_transcript" were considered to the matching lncRNA probe.

Finally, the probe numbers and mRNA/lncRNA (Gene symbol) were matched one by one to remove probes that did not match to Gene symbol. For different probes mapping to the same gene, we used the average of different probes as the final expression value of the mRNA/lncRNA.

4.3. Differential MRNA, lncRNA and MiRNA Screening

We took the R software limma package with the classical Bayesian method[10] (version 3.10.3, http://www.bioconductor.org/packages/2.9/bioc/html/limma.html). The differential analysis was performed between CAD and CTRL. Importantly, the miRNAs, mRNAs, and lncRNAs were analyzed to obtain their p values and logFC values, which were evaluated at the levels of both fold difference and statistical significance. The threshold of differential expression was set as miRNA: p value < 0.05 and |logFC| > 0.263 (>1.2 times).

4.4. Functional Enrichment and Pathway Analysis of Differentially Expressed MRNA

Enrichment analysis was performed with the common enrichment analysis tool DAVID[11] (version 6.8, https://david-d.ncifcrf.gov/) to analyze the up- and down- regulated genes, which were involved in the pathways of Gene Ontology BP (biological process),[12] CC (cellular component), MF (molecular function) and KEGG.[13] Significant enrichment results were considered to a significance threshold p value < 0.05 and an at least 2 of

Preprints (www.preprints.org) | NOT PEER-REVIEWED | Posted: 16 March 2020

enrichment number (count).

4.5. Protein Interaction Network (PPI) Construction and Node Connectivity Analysis

In combination with STRING (version: 10.0, http://www.string-db.org/),[14] the database predicted whether there was an interaction relationship between the proteins encoded by the analyzed genes. The differential mRNAs were inputted into gene sets, and homo was inputted into species. The parameter of PPI score was set to 0.9 (highest confidence), the interactional protein nodes were required in the up- and down- regulated genes. After the PPI relationship pairs were obtained, the data were analyzed using Cytoscape software (version 3.4.0, http://chianti.ucsd.edu/cytoscape-3.4.0/),[15] for which a network map was constructed. The node connectivity analysis was performed with parameters of no weigh by using the CytoNCA plugin (Version 2.1.6, http://apps.cytoscape.org/ apps/cytonca).[16] The results obtained the important nodes in the PPI network that were involved in protein interaction relationships, i.e., hub proteins, through the connectivity Degree Centrality (DC) rank of individual nodes.

4.6. lncRNA and MRNA Co-expression Analysis

The correlation test was performed and their pearson correlation coefficients of the differential mRNA and lncRNA were respectively calculated by using the matched sample of mRNA and lncRNA data. The relationship pairs with $r > 0.7$ (coordinate expression) and p value < 0.05 were focused on screening for the subsequent ceRNA network construction, and these mRNAs were considered to be significantly correlated with lncRNAs, while mRNAs were considered as potential target genes of lncRNAs.

4.7. Target Genes MiRNA and The Prediction for Their Upstream lncRNA

Based on the differential miRNAs obtained from the differential analysis, miRWalk2.0 (http://zmf.umm.uni-heidelberg.de/apps/zmf/mirwalk2/)

Preprints (www.preprints.org) | NOT PEER-REVIEWED | Posted: 16 March 2020

database[17] was used, which integrated the four typical databases including miRWalk, miRanda, RNA22, and TargetScan. If the predicted target genes were presented in each of four databases, the marching mRNA was considered to be regulated by the miRNA. After the predicted miRNA-mRNA relationship pairs were obtained, the mRNAs were further intersected with the differential mRNAs to obtain the differential miRNA-differential mRNA relationship pairs.

With regard to differential lncRNAs versus differential miRNAs, we used the local software miRanda (v3.3a)[18] to predict differential miRNA-differential lncRNA relationship pairs through software parameters (-sc140, -en-20, i.e., screen score > = 140, energy < = -20).

4.8. Pathway Enrichment Analysis of lncRNAs and MiRNAs

Based on the obtained lncRNA-mRNA co-expression relationship pairs and miRNA-mRNA relationship pairs, mRNAs were used as potential target genes of matching lncRNAs and miRNAs, respectively. KEGG Pathway enrichment analysis was performed by using the R package clusterProfiler (version: 3.8.1, http://bioconductor.org/packages/release/bioc/html/clusterProfiler.html),[19] and its results indirectly predicted the functions of lncRNAs and miRNAs. The threshold was set at p value < 0.05.

4.9. CeRNA Network Construction

Based on the obtained mRNA-miRNA and lncRNA-miRNA relationship pairs, we firstly screened the miRNA-lncRNA-mRNA relationship pairs regulated by the same miRNA, then combined the positive co-expression relationship between mRNA and lncRNA (correlation coefficient > 0.7), and further screened the miRNA-lncRNA-mRNA relationship pairs for network construction, i.e., the ceRNA network. Thus, the lncRNAs and mRNAs with positive co-expression relationship regulated by the same miRNA in the ceRNA network were each other ceRNAs.

Finally, the node connectivity (degree) analysis was also performed

Preprints (www.preprints.org) | NOT PEER-REVIEWED | Posted: 16 March 2020

using the Cytoscape plugin CytoNCA with the parameter set to no weight. The higher the connectivity, the higher the importance of this node in the network.

5. Conclusions

Based on eleven Go and KEGG pathways, top 15 of PPI network node connectivity rank, and top 15 of ceRNA network node degree centrality rank in CAD population, our findings would contribute to further exploration for the molecular mechanism of CAD.

Supplementary Materials: Supplementary tables can be found in supplementary Material

Authors' Contributions: Shen Kang conceived and designed the study, Shen Kang analyzed data and drafted the manuscript, Yong Ye participated in the data collection. Guang Xia was responsible for quality control and revised the manuscript, Haibo Liu analysis the data and participated in the fund support of the study.

Funding: This work was supported in part by Projects of National Natural Science Foundation of China (81870247, 81770350, 81800224); Key Disciplines Group Construction Project of Pudong Health Bureau of Shanghai (Grant No. PWZxq 2017-05), and Top-level Clinical Discipline Project of Shanghai Pudong District (Grant No. PWYgf 2018-02).

Acknowledgements: We sincerely appreciated Wei Song and Hong-Chun Fan for technical support in the study.

Abbreviations

BP	biological process
CAD	coronary artery disease
CARM1	Co-activator-associated arginine methyltransferase 1
CC	cellular component

Preprints (www.preprints.org) | NOT PEER-REVIEWED | Posted: 16 March 2020

ceRNA	competitive endogenous RNA
circRNA	circular RNA
CTRL	control
Cxcr4	C-X-C motif chemokine receptor 4
DC	degree centrality
ECs	endothelial cells
GPCR	G protein-coupled receptor
lncRNA	long-chain non-coding RNA
MF	molecular function
miRNAs	microRNAs
MRE	miRNA response element
mRNA	messenger RNA
OPCs	oligodendrocyte precursor cells
PPI	protein interaction network
STK35	Serine/threonine kinase 35

References

1. Cannon CP, Blazing MA, Giugliano RP, et al. Ezetimibe Added to Statin Therapy after Acute Coronary Syndromes. N Engl J Med 2015;372(25):2387-2397.

2. Karakas M, Schulte C, Appelbaum S, et al. Circulating microRNAs strongly predict cardiovascular death in patients with coronary artery disease-results from the large AtheroGene study. Eur Heart J 2017;38(7):516-523.

3. Graham MJ, Lee RG, Brandt TA, et al. Cardiovascular and Metabolic Effects of ANGPTL3 Antisense Oligonucleotides. N Engl J Med 2017;377(3):222-232.

4. Lo Sardo V, Chubukov P, Ferguson W, et al. Unveiling the Role of the Most Impactful Cardiovascular Risk Locus through Haplotype Editing. Cell 2018;175(7):1796-1810.

5. Salmena L, Poliseno L, Tay Y, Kats L, Pandolfi PP. A ceRNA hypothesis: the Rosetta Stone of a hidden RNA language? Cell 2011;146(3):353-358.

6. de Giorgio A, Krell J, Harding V, Stebbing J, Castellano L. Emerging roles of

Preprints (www.preprints.org) | NOT PEER-REVIEWED | Posted: 16 March 2020

competing endogenous RNAs in cancer: insights from the regulation of PTEN. Mol Cell Biol 2013;33(20):3976- 3982.

7. Barrett T, Suzek TO, Troup DB, et al. NCBI GEO: mining millions of expression profiles--database and tools. Nucleic Acids Res 2005;33(Database issue): D562-566.

8. Harrow J, Frankish A, Gonzalez JM, et al. GENCODE: the reference human genome annotation for The ENCODE Project. Genome Res 2012;22(9):1760-1774.

9. Jiang H, Wong WH. SeqMap: mapping massive amount of oligonucleotides to the genome. Bioinformatics 2008;24(20):2395-2396.

10. Smyth, G.K., limma: Linear Models for Microarray Data, in Bioinformatics and Computational Biology Solutions Using R and Bioconductor, R. Gentleman, et al., Editors. 2005, Springer New York: New York, NY. p. 397-420.

11. Huang da W, Sherman BT, Lempicki RA. Systematic and integrative analysis of large gene lists using DAVID bioinformatics resources. Nat Protoc 2009;4(1):44-57.

12. Ashburner M, Ball CA, Blake JA, et al. Gene ontology: tool for the unification of biology. The Gene Ontology Consortium. Nat Genet 2000;25(1):25-29.

13. Kanehisa M, Goto S. KEGG: kyoto encyclopedia of genes and genomes. Nucleic Acids Res 2000;28(1):27-30.

14. Szklarczyk D, Franceschini A, Wyder S, et al. STRING v10: protein-protein interaction networks, integrated over the tree of life. Nucleic Acids Res 2015;43 (Database issue): D447-D452.

15. Shannon P, Markiel A, Ozier O, et al. Cytoscape: a software environment for integrated models of biomolecular interaction networks. Genome Res 2003;13(11):2498-2504.

16. Tang Y, Li M, Wang J, Pan Y, Wu FX. CytoNCA: a cytoscape plugin for centrality analysis and evaluation of protein interaction networks. Biosystems 2015; 127:67-72.

17. Yu G, Wang LG, Han Y, He QY. clusterProfiler: An R package for comparing biological themes among gene clusters. OMICS. 2012;16(5):284-7.

18. Dweep H, Gretz N. miRWalk2.0: a comprehensive atlas of microRNA-target interactions. Nat

Preprints (www.preprints.org) | NOT PEER-REVIEWED | Posted: 16 March 2020

Methods 2015;12(8):697.

19. Enright AJ, John B, Gaul U, Tuschl T, Sander C, Marks DS. MicroRNA targets in Drosophila. Genome Biol 2003;5(1): R1.

20. Hossain MN, Sakemura R, Fujii M, Ayusawa D. G-protein gamma subunit GNG11 strongly regulates cellular senescence. Biochem Biophys Res Commun 2006;351(3):645-650.

21. Nolte IM, Munoz ML, Tragante V, et al. Genetic loci associated with heart rate variability and their effects on cardiac disease risk. Nat Commun 2017;8:15805.

22. Girbl T, Lenn T, Perez L, et al. Distinct Compartmentalization of the Chemokines CXCL1 and CXCL2 and the Atypical Receptor ACKR1 Determine Discrete Stages of Neutrophil Diapedesis. Immunity 2018;49(6):1062-1076.

23. Wang L, Zhang YL, Lin QY, et al. CXCL1-CXCR2 axis mediates angiotensin II-induced cardiac hypertrophy and remodelling through regulation of monocyte infiltration. Eur Heart J 2018; 39(20):1818-1831.

24. Tsai HH, Niu J, Munji R, et al. Oligodendrocyte precursors migrate along vasculature in the developing nervous system. Science 2016;351(6271):379-384.

25. Wang J, Hossain M, Thanabalasuriar A, Gunzer M, Meininger C, Kubes P. Visualizing the function and fate of neutrophils in sterile injury and repair. Science 2017;358(6359):111-116.

26. Döring Y, Noels H, van der Vorst EPC, et al. Vascular CXCR4 Limits Atherosclerosis by Maintaining Arterial Integrity: Evidence From Mouse and Human Studies. Circulation 2017;136(4):388-403.

27. Boström P, Andersson L, Rutberg M, et al. SNARE proteins mediate fusion between cytosolic lipid droplets and are implicated in insulin sensitivity. Nat Cell Biol 2007;9(11):1286-1293.

28. Shin HJ, Kim H, Oh S, et al. AMPK-SKP2-CARM1 signalling cascade in transcriptional regulation of autophagy. Nature 2016;534(7608):553-557.

29. Reyes-Resina I, Navarro G, Aguinaga D, et al. Molecular and functional interaction between GPR18 and cannabinoid CB2 G-protein-coupled receptors. Relevance in neurodegenerative diseases. Biochem Pharmacol 2018;157:169-179.

Preprints (www.preprints.org) | NOT PEER-REVIEWED | Posted: 16 March 2020

30. Matouk AI, Taye A, El-Moselhy MA, Heeba GH, Abdel-Rahman AA. The Effect of Chronic Activation of the Novel Endocannabinoid Receptor GPR18 on Myocardial Function and Blood Pressure in Conscious Rats. J Cardiovasc Pharmacol 2017;69(1):23-33.

31. Sun KY, Peng T, Chen Z, Song P, Zhou XH. Long non-coding RNA LOC100129148 functions as an oncogene in human nasopharyngeal carcinoma by targeting miR-539-5p. Aging (Albany NY) 2017;9(3):999-1011.

32. Wei JQ, Chen H, Zheng XF, et al. Hsa-miR-654-5p regulates osteogenic differentiation of human bone marrow mesenchymal stem cells by repressing bone morphogenetic protein 2. Nan Fang Yi Ke Da Xue Xue Bao 2012;32(3):291-295.

33. Liu Y, Lu C, Zhou Y, Zhang Z, Sun L. Circular RNA hsa_circ_0008039 promotes breast cancer cell proliferation and migration by regulating miR-432-5p/E2F3 axis. Biochem Biophys Res Commun 2018;502(3):358-363.

34. Xu H, Han H, Song S, et al. Exosome-Transmitted PSMA3 and PSMA3-AS1 Promote Proteasome Inhibitor Resistance in Multiple Myeloma. Clin Cancer Res 2019;25(6):1923-1935.

35. Thiebaut C1, Chesnel A2, Merlin JL, et al. Dual Epigenetic Regulation of ERα36 Expression in Breast Cancer Cells. Int J Mol Sci 2019;20(11). pii: E2637.

36. Watts AE, Millar NL, Platt J, et al. MicroRNA29a Treatment Improves Early Tendon Injury. Mol Ther 2017;25(10):2415-2426.

37. Bai X, Geng J, Li X, et al. Long Noncoding RNA LINC01619 Regulates MicroRNA-27a/Forkhead Box Protein O1 and Endoplasmic Reticulum Stress-Mediated Podocyte Injury in Diabetic Nephropathy. Antioxid Redox Signal 2018;29(4):355-376.

38. Shivakumar M, Lee Y, Bang L, Garg T, Sohn KA, Kim D. Identification of epigenetic interactions between miRNA and DNA methylation associated with gene expression as potential prognostic markers in bladder cancer. BMC Med Genomics 2017;10(Suppl 1):30.

39. Hasan MM, Akter R, Ullah MS, Abedin MJ, Ullah GM, Hossain MZ. A Computational Approach for Predicting Role of Human MicroRNAs in MERS-CoV

Preprints (www.preprints.org) | NOT PEER-REVIEWED | Posted: 16 March 2020

Genome. Adv Bioinformatics 2014;2014: 967946.

40. Zhang WC, Chin TM, Yang H, et al. Tumour-initiating cell-specific miR-1246 and miR-1290 expression converge to promote non-small cell lung cancer progression. Nat Commun 2016; 7:11702.

41. Schulz J, Takousis P, Wohlers I, et al. Meta-analyses identify differentially expressed micrornas in Parkinson's disease. Ann Neurol 2019;85(6):835-851.

42. Meng Y, Quan L, Liu A. Identification of key microRNAs associated with diffuse large B-cell lymphoma by analyzing serum microRNA expressions. Gene 2018; 642:205-211.

43. Wang W, Zhao Z, Yang F, et al. An immune-related lncRNA signature for patients with anaplastic gliomas. J Neurooncol 2018;136(2):263-271.

44. Goyal P, Behring A, Kumar A, Siess W. STK35L1 associates with nuclear actin and regulates cell cycle and migration of endothelial cells. PLoS One 2011;6(1): e16249.

45. Miyamoto Y, Whiley PAF, Goh HY, et al. The STK35 locus contributes to normal gametogenesis and encodes a lncRNA responsive to oxidative stress. Biol Open 2018;7(8). pii: bio032631.

46. Yasuda Y, Miyamoto Y, Yamashiro T, et al. Nuclear retention of import in α coordinates cell fate through changes in gene expression. EMBO J 2012;31(1):83-94.